Cholesterol Depletion Increases Membrane Stiffness of Aortic Endothelial Cells

Fitzroy J. Byfield,* Helim Aranda-Espinoza,* Victor G. Romanenko,* George H. Rothblat,† and Irena Levitan*
*Institute for Medicine and Engineering, Department of Pathology and Laboratory Medicine, University of Pennsylvania, Philadelphia, Pennsylvania; and †Lipid Research Group, The Children's Hospital of Philadelphia, Philadelphia, Pennsylvania

ABSTRACT This study has investigated the effect of cellular cholesterol on membrane deformability of bovine aortic endothelial cells. Cellular cholesterol content was depleted by exposing the cells to methyl-β-cyclodextrin or enriched by exposing the cells to methyl-β-cyclodextrin saturated with cholesterol. Control cells were treated with methyl-β-cyclodextrin-cholesterol at a molar ratio that had no effect on the level of cellular cholesterol. Mechanical properties of the cells with different cholesterol contents were compared by measuring the degree of membrane deformation in response to a step in negative pressure applied to the membrane by a micropipette. The experiments were performed on substrate-attached cells that maintained normal morphology. The data were analyzed using a standard linear elastic half-space model to calculate Young elastic modulus. Our observations show that, in contrast to the known effect of cholesterol on membrane stiffness of lipid bilayers, cholesterol depletion of bovine aortic endothelial cells resulted in a significant decrease in membrane deformability and a corresponding increase in the value of the elastic coefficient of the membrane, indicating that cholesterol-depleted cells are stiffer than control cells. Repleting the cells with cholesterol reversed the effect. An increase in cellular cholesterol to a level higher than that of normal cells, however, had no effect on the elastic properties of bovine aortic endothelial cells. We also show that although cholesterol depletion had no apparent effect on the intensity of F-actin-specific fluorescence, disrupting F-actin with latrunculin A abrogated the stiffening effect. We suggest that cholesterol depletion increases the stiffness of the membrane by altering the properties of the submembrane F-actin and/or its attachment to the membrane.

INTRODUCTION

Cholesterol is one of the main lipid components of the plasma membrane in all mammalian cells where phospholipids/cholesterol molar ratio may be as high as 1:1 (Yeagle, 1985). It is also well known that changes in the level of membrane cholesterol have a major impact on the physical properties of the membrane lipid bilayer, such as ordering of the phospholipids (e.g., Demel et al., 1972; Demel and De Kruyff, 1976; Stockton and Smith, 1976), changes in membrane fluidity (e.g., Brulet and McConnell, 1976; Cooper, 1978; Xu and London, 2000), and membrane elastic modulus, a measure of membrane deformability (Evans and Needham, 1987; Needham and Nunn, 1990). In living cells, however, membrane deformability depends strongly on submembrane cytoskeleton, which underlies the plasma membrane (Sato et al., 1990; Pourati et al., 1998; Wu et al., 1998; Rotsch and Radmacher, 2000; Zhang et al., 2002). In this study, therefore, we investigate the role of cholesterol in the deformability of membrane-cytoskeleton complex in substrate-attached endothelial cells.

Growing evidence suggests that cholesterol-rich membrane domains (lipid rafts), known to be enriched in cholesterol, sphyngomyelin, and a variety of signaling molecules (reviewed by Simons and Ikonen, 1997; Brown and London, 2000; Edidin, 2003), serve as focal points for coupling between the plasma membrane and the submembrane cytoskeleton. One, proteomic analysis shows that several cytoskeletal proteins, such as β-actin, fodrin, vimentin, as well as several actin-binding proteins are associated with lipid-raft membrane fractions (Nebl et al., 2002). Two, lipid rafts are enriched with a regulatory phospholipid PIP_2 (Pike and Miller, 1998; Laux et al., 2000; Caroni, 2001), which is known to modulate cytoskeleton/membrane interactions (Yin and Janmey, 2003). Three, caveolin-1, a major structural protein of caveolae, a subpopulation of lipid rafts, is associated with the F-actin cross-linking protein, filamin, suggesting that caveolae are associated with submembrane actin fibers (Stahlhut and van Deurs, 2000). In addition, Harder and Simons (Harder et al., 1997) showed that cholesterol depletion, a treatment that is known to disrupt lipid rafts (Brown and London, 2000), resulted in the dissociation of multiple cytoskeletal proteins from the membrane fractions. Taken together, these observations suggest that disruption of lipid rafts will dissociate the membrane from the cytoskeleton, resulting in a decrease of membrane stiffness and increase of its deformability. Our study, however, shows that cholesterol depletion increases rather than decreases membrane stiffness in aortic endothelial cells, as measured by micropipette aspiration. We suggest, therefore, that the integrity and/or membrane coupling of F-actin is stabilized by cholesterol depletion. This is the first study to show that the stiffness of cellular membrane increases upon cholesterol depletion.

Submitted January 22, 2004, and accepted for publication August 23, 2004.

Address reprint requests to Irena Levitan, 3340 Smith Walk, Philadelphia, PA 19104. Tel.: 215-573-8161; Fax: 215-573-7227; E-mail: ilevitan@mail.med.upenn.edu.

0006-3495/04/11/3336/08 $2.00

doi: 10.1529/biophysj.104.040634

METHODS

Cell culture

Bovine aortic endothelial cells (BAECs) between passages 10 and 30 were grown in Dulbecco's Modified Eagle's Medium (DMEM; Cell Grow, Washington, DC) supplemented with 10% bovine serum (Gibco BRL, Grand Island, NY). Cell cultures were maintained in a humidified incubator at 37°C with 5% CO_2. The cells were fed and split every 3–4 days.

Modulation of cellular cholesterol level and measurement of cellular cholesterol content

BAECs were enriched with or depleted of cholesterol by incubating them with methyl-β-cyclodextrin (MβCD) saturated with cholesterol or with empty MβCD (not complexed with cholesterol), as described in our previous studies (e.g., Levitan et al., 2000). Free cholesterol mass analysis was done by gas-liquid chromatography (GLC) (as described in e.g., Levitan et al., 2000), and the phospholipid content was determined using a modified phosphorous assay (Sokoloff and Rothblat, 1974). Cell protein was determined on the lipid-extracted monolayer using a modification of the method of Lowry et al. (1951). All mass values were normalized on the basis of cell protein.

Micropipette aspiration (microaspiration)

The membranes of substrate-attached cells were aspirated using micropipettes with 3–5 μm outer diameter pulled from borosilicate glass capillaries (SG10 glass; Richland Glass, Richland, NJ). The pipettes were filled with a saline solution (PBS) with 30% calf serum, the latter used as a lubricant to allow the membrane to move into the pipette. The use of calf serum or BSA is a standard procedure in these types of experiments (Discher et al., 1994; Griffin et al., 2004).

Modification of micropipette aspiration for substrate-attached cells

In earlier studies, micropipette aspiration was performed either on liposomes (Needham and Nunn, 1990) or on cells that were not attached to the substrate (Chien et al., 1978; Evans and Kuhan, 1984; Theret et al., 1988; Needham and Nunn, 1990; Sato et al., 1990; Discher et al., 1994). In our study, however, the cells were maintained attached to the substrate to avoid changes in the cytoskeletal structure that are likely to occur when cells detach. Therefore, during aspiration, the pipette could not be positioned horizontally, as was done in the previous studies to allow the aspirated membrane to remain in a single focal plane. Therefore, in our experiments, the shank of the pipette was aligned horizontally to the bottom of the chamber by 1), positioning the pipette at the shallowest angle possible (10–15°); and 2), by flexing the shank of the pipette against the bottom of the chamber, as shown schematically in Fig. 1 *A* (the *inset* demonstrates the inner and the outer diameters, the two parameters used in the deformation analysis). A typical bright contrast image of a pipette touching an endothelial cell is shown in Fig. 1 *B*. Fig. 1 *C* shows the fluorescent image of the same cell when the plasma membrane is visualized with a fluorescent membrane dye carbocyanide $DiIC_{18}$ (DI, Molecular Probes, Eugene, OR). The cells were incubated with 5 μM of $DiIC_{18}$, for 30 min before aspiration experiments. In this image the pipette is invisible because it is non-fluorescent before the beginning of aspiration. The fluorescent images were acquired using a Zeiss Axiovert 100TV microscope (Zeiss, Jena, Germany) with 40× Plan-Apochromat lens (NA 0.75), and a scientific-grade cooled CCD camera (MicroMax, Princeton Instruments, Trenton, NJ). All cells taken for microaspiration experiments were of similar elongated shape, typical for viable endothelial cells in subconfluent cell culture.

F-actin staining

F-actin staining was performed using a standard procedure. Briefly, the cells were fixed in 4% paraformaldehyde PFA for 20 min, permeabilized with 0.1% Triton-X100 for 5 min, and incubated with 0.1 μM Rhodamine-Phalloidin (Sigma, St. Louis, MO) for 40 min. The images were acquired using the same optical system, as described for microaspiration experiments using 63× Plan-Apochromat lens (NA 1.4).

Analysis

To quantify the degree of membrane deformation, the equilibrium aspirated length (L) was measured from the tip of the pipette to the vertex of the circumference of the membrane projection. The measurements were performed using Delta Vision SoftWorx software package (Applied Precision, Issaquah, WA). For each individual cell, the aspirated length was plotted as a function of the applied pressure. In most cases, we observed a linear behavior. The data was fit to the equation $P = K^{L}/_{a} + P_0$ (Hochmuth, 2000) using least-squares fit, where P is the applied negative pressure, K is the slope of the curve, L is the length of the membrane projection into a pipette of internal radius a, and P_0 represents the prestress. The value of K is a measure of the elastic properties of the system, where large K represents a stiff material whereas a small K represents a soft material.

The data was further analyzed using the infinite homogenous half-space model developed by Theret et al. (1988) where the endothelial cell is modeled as a homogenous, incompressible elastic half space. In this model, the applied negative pressure from the pipette is taken as a tensile stress over a circular region, which is equilibrated by the stresses in the annular region of contact between pipette and membrane. To simplify the model, the origin of the coordinate system is situated at the center of the pipette and the system is assumed to be axisymmetric. This model represents only a rough approximation to the mechanical behavior of a substrate-attached cell that is finite, nonhomogenous, and has complicated morphology. The Young modulus obtained in our calculations serves only to compare it with the other studies using a similar model. The effective Young's modulus of the cells (E) in Theret et al. (1988), model is given as:

$$E = \frac{3a\Delta p}{2\pi L}\,\phi(\eta), \tag{1}$$

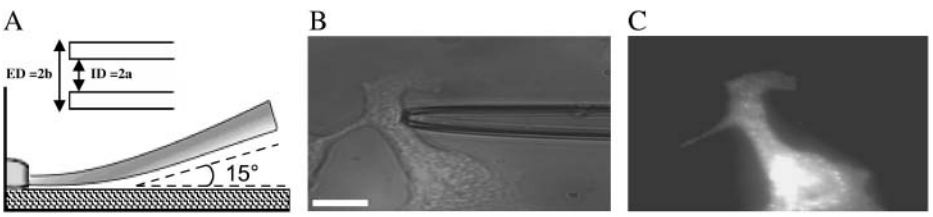

FIGURE 1 Micropipette aspiration technique for substrate attached BAECs. (*A*) Schematic side view of a micropipette approaching a substrate-attached cell. Inset, depiction of micropipette parameters used in analysis, where $ID = 2a$ = internal diameter and $ED = 2b$ = external diameter. (*B*) Bright contrast image of a micropipette shank touching a typically shaped cell used in aspiration experiments. (*C*) Fluorescent image of the same cell labeled with $DiIC_{18}$. The micropipette is still present but is invisible. Scale bar, 30 μm.

where Δp is the applied pressure difference, $\phi(\eta)$ is the wall function that is defined by the boundary condition at the contact zone between the cell and the micropipette, $\eta = (b - a)/a$, and b is the external pipette radius. Theret et al. (1988) defined two sets of boundary conditions, which are known as the force and punch models. Both models give a similar expression for the effective Young's modulus with only a different multiplying function $\phi(\eta)$ (Theret et al., 1988). In our calculations, we have used the force model whereas the alternative (punch model) gives only small quantitative differences in the values of the effective Young's modulus with the same qualitative behavior. Substituting the expressions for K (with $P_0 = 0$) into the equation for the Young' modulus we get:

$$E = \frac{3\phi((b-a)/a)}{2\pi} K. \quad (2)$$

This latter equation is used to calculate the Young's modulus in our study. It is noteworthy, however, that the values of the Young's modulus calculated in our study are similar to the values reported by Theret et al. (1988). Finally, the applied pressure could also involve volumetric changes of the system, i.e., the cell and/or the membrane. Although the thickness could not be measured in these experiments, the assumption that the cell volume is constant is based on the observation that the projected cell surface area does not change during aspiration. Thus, although this model represents a rough approximation given the highly complex cell morphology and the heterogeneity of the plasma membrane and the cell cytoplasm, we suggest that it is appropriate at this stage to assume that no volumetric changes occurred during the aspiration experiments.

RESULTS

Validation of the microaspiration technique for substrate-attached BAECs using F-actin disruption

Earlier studies have shown that membrane deformability of BAECs detached from the substrate depend strongly on the integrity of F-actin (Sato et al., 1990). To validate the use of microaspiration technique to detect changes in the mechanical properties of substrate-attached cells, we have verified that the same effect is observed in substrate-attached BAECs. The cells were exposed to 2 μM latrunculin A, a toxin that is known to depolymerize F-actin (Spector et al., 1989). As expected, less actin fibers were observed in latrunculin A-treated cells (*inset* to Fig. 2). Disruption of F-actin resulted in a significant increase in the length of membrane projections under the same negative pressure (Fig. 2). Application of increasing negative pressure through a micropipette results in a progressive deformation of the membrane with time (Fig. 2

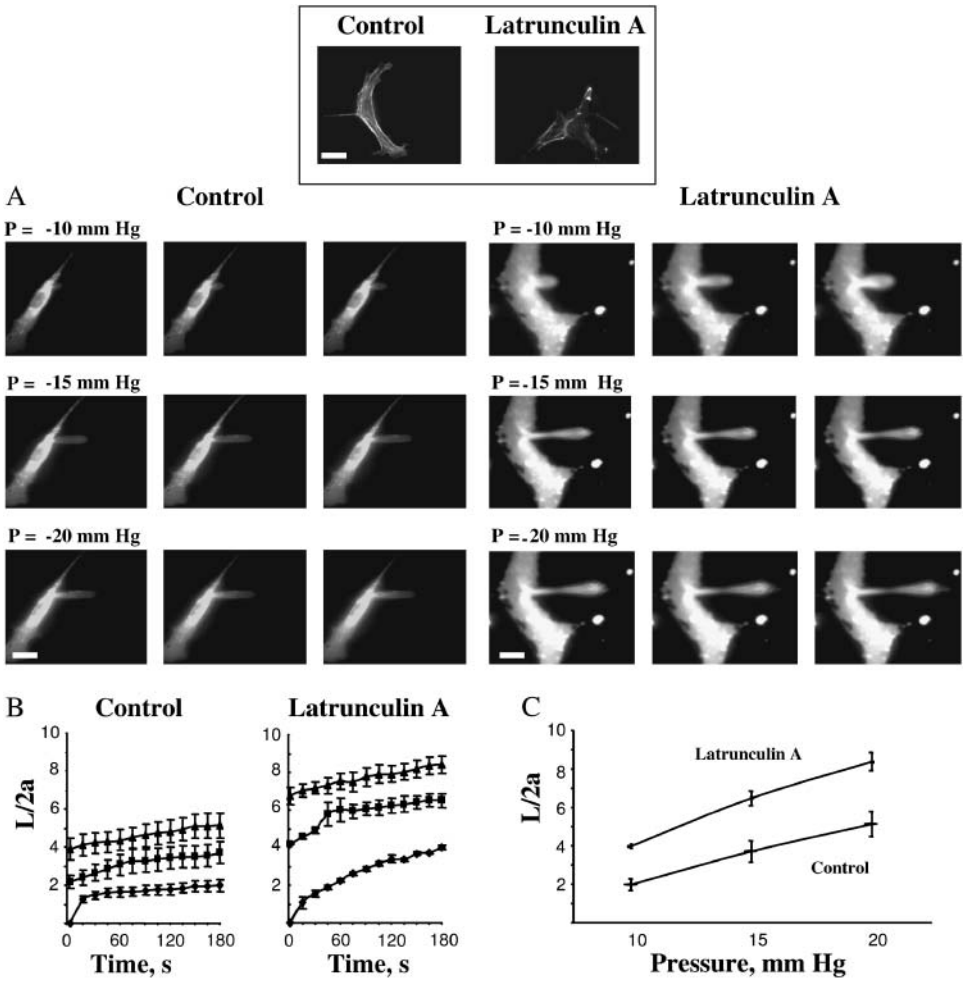

FIGURE 2 Membrane deformation of substrate-anchored endothelial cells under control conditions and after being exposed to latrunculin A. (*Inset*) The effect of latrunculin A on F-actin filaments visualized with rhodamine phalloidin. The bright spots in phalloidin staining were observed in most of the images suggesting that the treatment may result in collapse and condensation of actin fibers. The bar is 25 μm. (*A*) Progressive deformation of control cells compared to that of cells exposed to 2μM latrunculin A for 10 minutes. The edges of the cells have dimmer fluorescence than cell centers because in the cell center fluorescent signal comes not only from the plasma membrane but also from endocytosed vesicles. (*B*) Time course of membrane deformation where L is the aspirated length of the membrane projection and $2a$ is the inner diameter of the pipette. Cells were aspirated at -10 mm Hg (♦), -15 mm Hg (■), and -20 mm Hg (▲). (*C*) Maximal membrane deformation as a function of applied pressure. Maximal deformation was determined by taking the values at which the aspiration length plateaued for each pressure. The maximal normalized length in latrunculin treated cells was significantly greater than control cells for all pressures ($P < 0.05$).

A). The time courses and the pressure dependence of deformation show that disruption of F-actin significantly increases the aspirated lengths of the projections under all pressure conditions (Fig. 2, *B* and *C*). Similar results were obtained when BAECs were exposed to cytochalasin D, another F-actin depolymerizing agent (not shown). In summary, comparing the deformability of latrunculin-treated and control cells clearly shows that the stiffness of the cells is significantly reduced after the latrunculin treatment, consistent with previous studies (Sato et al., 1990).

Cholesterol depletion decreases membrane deformability of BAECs

The cells were exposed to a cyclic oligosaccharide MβCD or to MβCD saturated with cholesterol, as described in our earlier studies (Levitan et al., 2000). As was shown in our previous studies (Levitan et al., 2000; Romanenko et al., 2002), exposure of BAECs to MβCD alone decreased the level of cellular free cholesterol ~2-fold whereas exposure to MβCD saturated with cholesterol had the opposite effect (*inset* to Fig. 3). To exclude the possibility that the observed effects result from the exposure to MβCD itself, the cells were also exposed to MβCD/MβCD-cholesterol mixture (1:1 ratio), in which case the level of cellular cholesterol was identical to that of untreated cells. The level of free cholesterol under all experimental conditions was virtually identical to the level of total cholesterol (not shown) confirming our earlier observations that in aortic endothelial cells cholesterol exists almost completely in its free nonesterified form (Levitan et al., 2000). None of the treatments affected the level of cellular phospholipids (not shown).

Unexpectedly, a decrease in membrane cholesterol resulted in an increase in membrane stiffness, as measured by the aspirated length of membrane projection, whereas cholesterol enrichment had no significant effect (Fig. 3). The images show a cholesterol-enriched cell, a control cell, and a cholesterol-depleted cell after reaching maximal aspiration lengths at −15 mm Hg (Fig. 3 *A*). The projections typically started to develop at −10 mm Hg and the time courses of membrane deformation could be measured for the negative pressures of −10, −15, and −20 mm Hg (Fig. 3 *B*). Application of pressures above −25 mm Hg resulted in detachment of the aspirated projection forming a separate vesicle. The pressure level that resulted in membrane detachment was similar under different cholesterol conditions. Although no significant effect of cholesterol depletion was observed at −10 mm Hg, the difference between cholesterol-depleted and cholesterol-enriched cells became significant as the pressure was increased (Fig. 3 *C*). Control cells were exposed to MβCD/MβCD-cholesterol (1:1), so that the cells in all three experimental populations were exposed to the same concentration of MβCD.

When the levels of cellular cholesterol were replenished by incubating cholesterol-depleted cells with MβCD saturated with cholesterol (*inset* to Fig. 4), membrane elastic properties were fully recovered (Fig. 4).

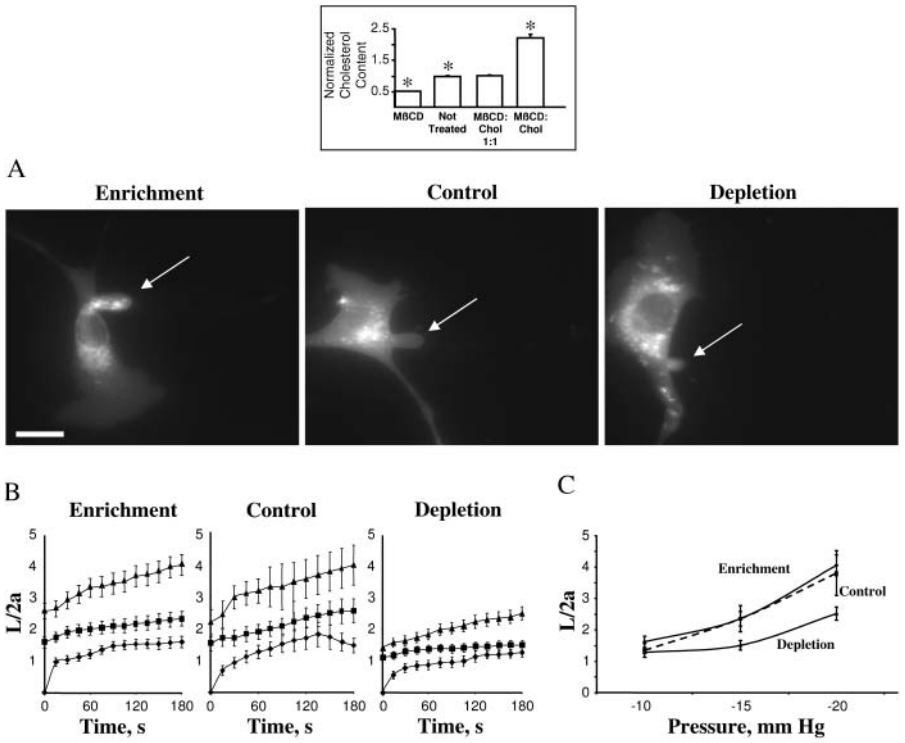

FIGURE 3 Effect of cellular cholesterol levels on membrane deformation of BAECs. (*Inset*) Effects of MβCD and MβCD-cholesterol on the levels of free cholesterol in BAECs. (*A*) Typical images of membrane deformation of cholesterol-enriched, cholesterol-depleted, and control cells (control cells were exposed to MβCD/MβCD-cholesterol mixture at 1:1 ratio that had no effect on the level of free cholesterol in the cells (see *inset*). The images shown depict the maximal deformation at −15 mm Hg. The arrow indicates the position of the aspirated projection. The bar is 30 μm. (*B*) Average time courses of aspirated lengths for the three experimental cell populations. (*C*) Maximal aspirated lengths plotted as a function of the applied pressure. The maximal normalized length in depleted cells was significantly lower than that of control cells for pressures −15 mm Hg and −20 mm Hg ($P < 0.05$).

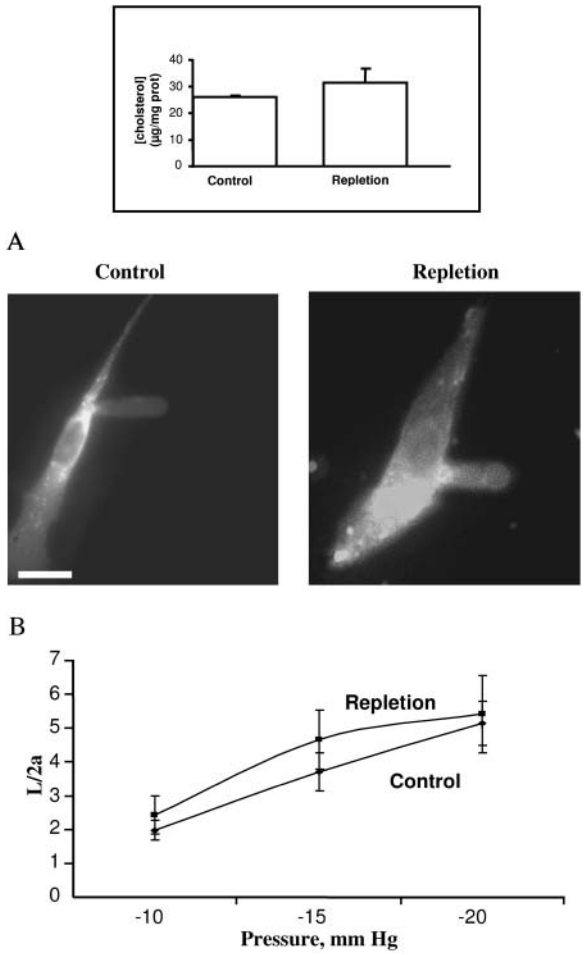

FIGURE 4 Effect of repletion on membrane deformation. (*Inset*) Free cholesterol level of cells after cholesterol repletion compared to that of control cells. (*A*) Typical images of the maximal deformation of a typical repleted cell (*left*) compared to that of a control cell (*right*) at −15 mm Hg. The bar is 25 μm. (*B*) Maximal normalized aspirated length as a function of pressure for repleted and control cells. Repleted cells ($n = 12$), Control cells ($n = 14$). There was statistically no difference between the two conditions.

Effect of cholesterol depletion on membrane deformability is abrogated by disruption of F-actin

Earlier studies have shown that in sperm cells, cholesterol efflux results in F-actin polymerization (Brener et al., 2003). In BAECs, however, there was no apparent increase in F-actin-specific staining indicating that accumulation of F-actin does not account for the observed increase in membrane stiffness in cholesterol-depleted BAECs (Fig. 5 *A*).

Importantly, although cholesterol depletion had no effect on F-actin-specific staining, disruption of F-actin with latrunculin A completely abrogated the stiffening effect of cholesterol depletion. Membrane deformation was compared in cholesterol-depleted and control cells, when both cell populations were exposed to 2 μM latrunculin A (Fig. 5 *B*). In this series of experiments, both control and cholesterol-depleted cells were more sensitive to the application of the pressure than cells in our previous experiments, so that the membrane was easily deformed at −5 mm Hg and the membrane projections detached when the pressure was increased further. It is important to note, however, that the length of the membrane projections obtained in this series of experiments in response to −5 mm Hg was similar to the length of the projections obtained in cells that were not treated with latrunculin in response to −15 mm Hg. These experiments indicate that integrity of F-actin is important for the stiffening effect of cholesterol depletion.

Comparison of the elastic parameters of BAECs under different cholesterol conditions

Typical plots of Δp versus L/a plots for three individual cells, cholesterol-depleted, cholesterol-enriched, and control cells, are shown in Fig. 6 *A*. The figure shows that a much larger pressure has to be applied to the cholesterol-depleted cell to achieve the same level of membrane deformation, indicating that cholesterol-depleted cells are stiffer than the other two experimental cell populations. The slopes of the curves for the individual cells of the three experimental cell populations (7 control, 10 cholesterol-enriched, and 17 cholesterol-depleted cells) were calculated as described in the Analysis section of Methods yielding the average values of 326 Pa, 323 Pa, and 536 Pa for control, cholesterol-enriched, and cholesterol-depleted cell populations respectively (Fig. 6 *B*). The *K* value for cholesterol-depleted cells was significantly higher than the K values for control and cholesterol-enriched cells ($P < 0.05$, Student's *t*-test), whereas no difference is observed between cholesterol-enriched and control cells. Fig. 6 *C* shows the values for the Young's modulus calculated for the same experimental cell populations using the approximation of infinite homogeneous half-space model, as described above. As expected, the value of the effective Young's modulus in cholesterol-depleted cells was significantly higher than in the other two experimental populations.

DISCUSSION

The main finding of this study is that cholesterol depletion increases the stiffness of aortic endothelial cells whereas cholesterol enrichment has no effect on membrane stiffness. We also show that the stiffening effect of cholesterol depletion depends on the integrity of F-actin. These observations suggest that in BAECs, disruption of lipid rafts by cholesterol depletion strengthens the mechanical scaffold of the plasma membrane, rather than uncouples the membrane from the submembrane cytoskeleton.

Plasma membranes of eukaryotic cells can be viewed as a bicomponent system where membrane lipid bilayer is underlied by the submembrane cytoskeleton. Earlier studies have shown that elevation of membrane cholesterol increases the stiffness of membrane lipid bilayers in artificial membrane vesicles (Needham and Nunn, 1990). Although the values for

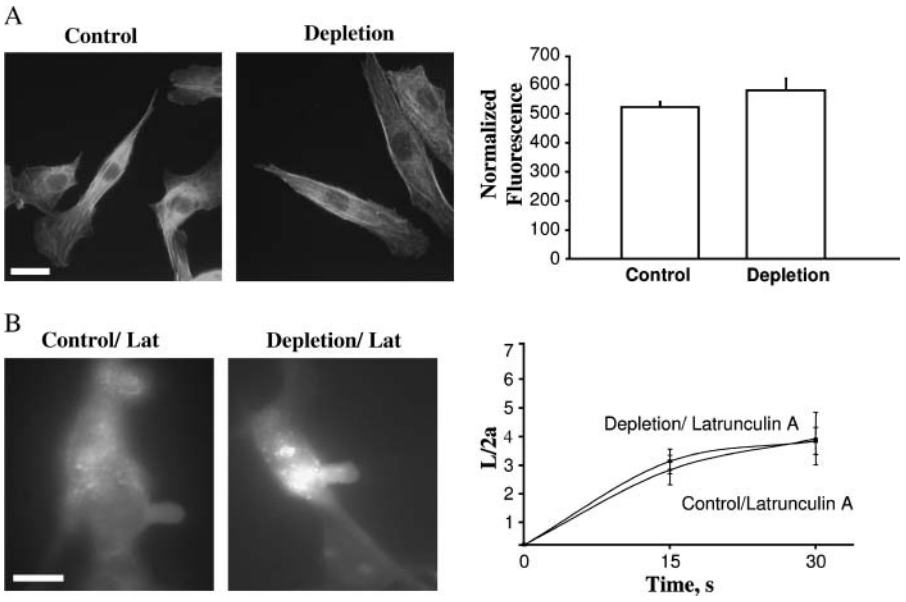

FIGURE 5 The role of F-actin in the stiffening effect of cholesterol depletion. (*A*) Effect of cholesterol depletion on F-actin specific staining. (*Left panel*) Rhodamine-phalloidin labeling of F-actin in control cells and cholesterol-depleted cells. (*Right panel*) Average fluorescence intensity of rhodamine phalloidin-labeled F-actin in control ($n = 20$) and depleted cells ($n = 20$) in a single experiment. There was no significant difference in intensity between depleted and control cells. Identical results were obtained in four independent experiments. (*B*) Effect of latrunculin A on the membrane deformation of control and cholesterol-depleted cells. (*Left panel*) Images of maximal deformation of a control and a cholesterol-depleted cell after being treated with latrunculin A. These images were acquired after 30 s at −5 mm Hg. The bar is 30 μm. (*Right panel*) Average time courses of control ($n = 5$) and depleted cells ($n = 4$) aspirated at −5 mm Hg. Only 30 s of the time course was analyzed because most cells broke beyond this point.

membrane area expansivity modulus calculated by Needham and Nunn cannot be compared directly to the Young's modulus calculated in our experiments, as the calculations are model-dependent, it is possible to compare the effects qualitatively. The main parameter relating Young's modulus, bending modulus, and area compression modulus is the thickness of the membrane. In our case, the membrane is a highly complex system of unknown thickness, which is formed by a lipid bilayer and a cytoskeleton cortex. However, estimating the elastic modulus by the slope of the curve of membrane tension plotted as a function of membrane area expansion roughly corresponds to the stiffness parameter calculated in our study as the slope of pressure plotted as a function of the length of membrane projection. Therefore, although direct numerical comparison is complicated and ambiguous, the fact that the effects of cholesterol on the two slopes were opposite indicates that an increase in membrane stiffness in cholesterol-depleted cells observed in our study is definitely not due to its effect on the membrane lipid bilayer. We conclude, therefore, that an increase in membrane stiffness in cholesterol-depleted cells is due to changes in the properties of the submembrane cytoskeleton or its association with the membrane. It is important to note that the values of the Young's modulus obtained in this study are similar to those reported in earlier studies for BAECs detached from the substrate (Theret et al., 1988) indicating that although the homogeneous half-space model represents only an approximation to the elastic behavior of substrate-attached cells, it provides a useful framework for the analysis of our results. Our conclusion is consistent with the earlier studies showing that in living cells membrane deformability depends more on the properties of the submembrane cytoskeleton and its attachment to the membrane than on the physical properties of the lipid bilayer (Sato et al., 1990; Pourati et al., 1998; Wu et al., 1998; Rotsch and Radmacher, 2000; Zhang et al., 2002).

The most important and unexpected finding of our study is that cholesterol depletion results in stiffening of membrane-cytoskeleton complex, whereas the prediction from most of the previous studies would have been that cholesterol depletion is expected to decrease the stiffness of the complex. Indeed, if lipid rafts constitute the focal points for cytoskeleton attachment, disruption of the rafts would be expected to weaken the coupling and result in cytoskeleton detachment. This prediction was based on the earlier studies showing that cholesterol depletion resulted in the release of actin and several actin-binding proteins from these fractions (Harder et al., 1997), and that aggregation of lipid rafts induced actin accumulation associated with the aggregates (Harder and Simons, 1999). The actual measurement of membrane deformability in cholesterol-depleted BAECs, however, contradicts this prediction. It is also noteworthy that in these experiments, we use a relatively low concentration of MβCD, a cholesterol-depleting agent, removing not more than 50% cholesterol. We have shown earlier that under these conditions, there is no increase in nonspecific ion fluxes, indicating that plasma membrane integrity is not compromised (Levitan et al., 2000; Romanenko et al., 2002).

Interestingly, a recent study by Kwik et al. (2003) has shown that cholesterol depletion decreases the lateral diffusion of transmembrane proteins and that disruption of F-actin abrogates this effect. The authors suggested that cholesterol depletion stabilizes the submembrane cytoskeleton. Our study is consistent with this hypothesis and provides the first direct evidence that membrane deformability of aortic endothelium decreases with cholesterol depletion.

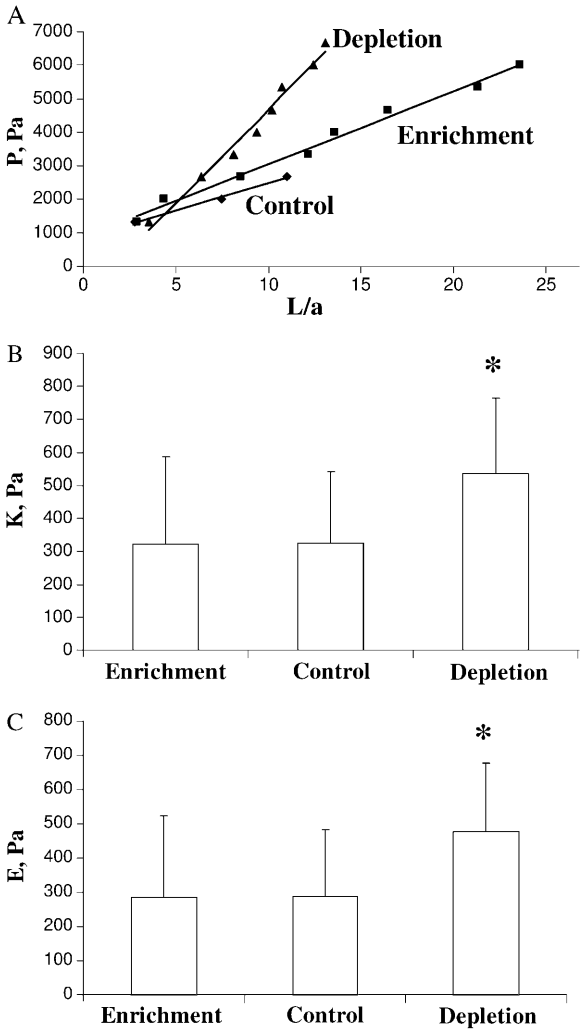

FIGURE 6 Analysis of the elastic properties of BAECs under different cholesterol conditions. (*A*) Typical data of the dimensionless aspirated projection length, L/a, as a function of the negative applied pressure difference, P, for control, cholesterol-enriched, and cholesterol-depleted cells with their respective least-squares fit (*solid lines*). (*B*) Elastic modulus K for control (7 cells), enrichment (10 cells), and depletion (17 cells) as obtained by least-squares fit of a straight line to the data. Depleted cells are significantly stiffer ($P < 0.05$) than control and cholesterol-enriched cells. Mean ± SE. (*C*) Young's modulus E according to the homogeneous half-space model (Eq. 1) for the data shown in *B*. Depleted cells have a significantly larger Young's modulus ($P < 0.05$) than control and cholesterol-enriched cells. Mean ± SE.

We demonstrate further that the stiffening effect of cholesterol depletion is abrogated by disruption of F-actin with latrunculin A. However, it is important to note that even in the presence of latrunculin A, plasma membranes still are likely to have multiple cytoskeleton proteins attached. It is not expected, therefore, that in the presence of latrunculin, plasma membranes will behave like pure lipid bilayers. In contrast, a lack of cholesterol effect on membrane stiffness of latrunculin-treated cells suggests that membrane stiffness in these cells is still dominated by cytoskeleton and that cholesterol depletion does not have the stabilization effect when F-actin is disrupted. It is apparent from our observations that the role of cholesterol in coupling between the cortical cytoskeleton and the plasma membrane is more complex than just providing focal points to cytoskeleton attachments. There are several molecular mechanisms that may be responsible for the observed effect. One possibility is that cholesterol depletion initiates actin polymerization creating more F-actin fibers, as was demonstrated in sperm where cholesterol efflux is a prerequisite of F-actin polymerization during sperm capacitation (Brener et al., 2003). We show, however, that in endothelial cells this is not the case because cholesterol depletion had no effect on the intensity of F-actin-specific staining or F-actin cellular distribution. There are multiple ways of how cholesterol depletion may affect the coupling of F-actin to the plasma membrane. For example, one possibility is that cholesterol depletion may affect actin stability by sequestering of PIP_2, as was suggested Kwik et al. (2003). Another possibility is that the effect is regulated by Rho-GTPases that have been reported to partition into lipid rafts (Grimmer et al., 2002). Possible contributions of these mechanisms to the observed increase in membrane stiffness of BAECs will be addressed in our future studies.

Since membrane-cytoskeleton coupling is central to a plethora of cellular responses, it is hard to overestimate the physiological significance of the cholesterol role in this coupling. Indeed, it has been shown that cholesterol depletion results in the impairment of several cytoskeleton-dependent cellular functions, such as motility of breast cancer-derived cells (Manes et al., 1999) and T cells (Gomez-Mouton et al., 2001), and polarization and migration of neutrophils (Pierini et al., 2003). It is important that these effects may be not only a direct result of lipid raft disruption but may also be the consequences of lipid raft-dependent changes in the cytoskeleton properties.

We thank Drs. Dennis Discher and Maureen Sheehan for helping us to learn the micropipette aspiration technique. We thank Drs. Peter Davies and Makoto Funaki for interesting and stimulating discussions and Dr. Yoram Lanir for the critical reading of the manuscript. We are also grateful to Mr. Gregory Kowalsky for preparing the cartoon for Fig. 1. A preliminary report describing the effect of cholesterol on membrane deformation of endothelial cells has been published as an extended abstract (Proc. IASTED International Conference. *Biomechanics*. June. 86–91).

This work was supported by the American Heart Association Scientist Development grant 0130254N and HL073965-01 (to I.L.), and the National Institutes of Health grants HL22633 and HL63768 (to G.R.), HL67286 (to Dr. Paul Janmey), and HL64388-01A1 and PO1-HL-622-50 (to Dr. Peter Davies).

REFERENCES

Brener, E., S. Rubinstein, G. Cohen, K. Shternall, J. Rivlin, and H. Breitbart. 2003. Remodeling of the actin cytoskeleton during mammalian sperm capacitation and acrosome reaction. *Biol. Reprod.* 68:837–845.

Brown, A. D., and E. London. 2000. Structure and function of sphingolipid- and cholesterol-rich membrane rafts. *J. Biol. Chem.* 275:17221–17224.

Brulet, P., and H. M. McConnell. 1976. Lateral hapten mobility and immunochemistry of model membranes. *Proc. Natl. Acad. Sci. USA.* 73: 2977–2981.

Caroni, P. 2001. New EMBO members' review: actin cytoskeleton regulation through modulation of PI(4,5)P(2) rafts. *EMBO J.* 20:4332–4336.

Chien, S., K. L. Sung, R. Skalak, S. Usami, and A. Tozeren. 1978. Theoretical and experimental studies on viscoelastic properties of erythrocyte membrane. *Biophys. J.* 24:463–487.

Cooper, R. A. 1978. Influence of increased membrane cholesterol on membrane fluidity and cell function in human red blood cells. *J. Supramol. Struct.* 8:413–430.

Demel, R. A., K. R. Bruckdorfer, and L. L. M. van Deenen. 1972. The effect of sterol structure on the permeability of liposomes to glucose, glycerol and Rb^+. *Biochim. Biophys. Acta.* 255:321–330.

Demel, R. A., and B. De Kruyff. 1976. The function of sterols in membranes. *Biochim. Biophys. Acta.* 457:109–132.

Discher, D. E., N. Mohandas, and E. A. Evans. 1994. Molecular maps of red cell deformation: hidden elasticity and *in situ* connectivity. *Science.* 266:1032–1035.

Edidin, M. 2003. The state of lipid rafts: from model membranes to cells. *Annu. Rev. Biophys. Biomol. Struct.* 32:257083.

Evans, E., and B. Kuhan. 1984. Passive material behavior of granulocytes based on large deformation and recovery after deformation tests. *Blood.* 64:1028–1035.

Evans, E., and D. Needham. 1987. Physical properties of surfactant bilayer membranes: thermal transition, elasticity, rigidity, cohesion and colloidal interactions. *J. Phys. Chem.* 91:4219–4228.

Gomez-Mouton, C., J. L. Abad, E. Mira, R. A. Lacalle, E. Gallardo, S. Jimenez-Baranda, I. Illa, A. Bernad, S. Manes, and C. Martinez-A. 2001. From the cover: segregation of leading-edge and uropod components into specific lipid rafts during T cell polarization. *Proc. Natl. Acad. Sci. USA.* 98:9642–9647.

Griffin, M. A., A. J. Engler, T. A. Barber, K. E. Healy, H. L. Sweeney, and D. E. Discher. 2004. Patterning, prestress, and peeling dynamics of myocytes. *Biophys. J.* 86:1209–1222.

Grimmer, S., B. van Deurs, and K. Sandvig. 2002. Membrane ruffling and macropinocytosis in A431 cells require cholesterol. *J. of Cell Sci.* 115:2953–2962.

Harder, T., R. Kellner, R. G. Parton, and J. Gruenberg. 1997. Specific release of membrane-bound annexin II and cortical cytoskeleton elements by sequestration of membrane cholesterol. *Mol. Biol. Cell.* 8:533–545.

Harder, T., and K. Simons. 1999. Clusters of glycolipid and glycosylphosphatidylinositol-anchored proteins in lymphoid cells: accumulation of actin regulated by local tyrosine phosphorylation. *Eur. J. Immunol.* 29:556–562.

Hochmuth, R. M. 2000. Micropipette aspiration of living cells. *J. Biomech.* 33:15–22.

Kwik, J., S. Boyle, D. Fooksman, L. Margolis, M. P. Sheetz, and M. Edidin. 2003. Membrane cholesterol, lateral mobility, and the phosphatidylinositol 4,5-biphosphate-dependent organization of cell actin. *Proc. Natl. Acad. Sci. USA.* 100:13964–13969.

Laux, T., K. Fukami, M. Thelen, T. Golub, D. Frey, and P. Caroni. 2000. GAP43, MARCKS, and CAP23 modulate PI(4,5)P(2) at plasmalemmal rafts, and regulate cell cortex actin dynamics through a common mechanism. *J. Cell Biol.* 149:1455–72.

Levitan, I., A. E. Christian, T. N. Tulenko, and G. H. Rothblat. 2000. Membrane cholesterol content modulates activation of volume-regulated anion current (VRAC) in bovine endothelial cells. *J. Gen. Physiol.* 115:405–416.

Lowry, O. H., N. Rosenbrough, A. Farr, and R. Randall. 1951. Protein measurements with folin phelon reagent. *J. Biol. Chem.* 193:265–275.

Manes, S., E. Mira, C. Gomez-Mouton, R. A. Lacalle, P. Keller, J. P. Labrador, and A. C. Martinez. 1999. Membrane raft microdomains mediate front-rear polarity in migrating cells. *EMBO J.* 18:6211–6220.

Nebl, T., K. N. Pestonjamasp, J. D. Leszyk, J. L. Crowley, S. W. Oh, and E. J. Luna. 2002. Proteomic analysis of a detergent-resistant membrane skeleton from neutrophil plasma membranes. *J. Biol. Chem.* 277:43399–43409.

Needham, D., and R. S. Nunn. 1990. Elastic deformation and failure of lipid bilayer membranes containing cholesterol. *Biophys. J.* 58:997–1009.

Pierini, L. M., R. J. Eddy, M. Fuortes, S. Seveau, C. Casulo, and F. R. Maxfield. 2003. Membrane lipid organization is critical for human neutrophil polarization. *J. Biol. Chem.* 278:10831–10841.

Pike, L. J., and J. M. Miller. 1998. Cholesterol depletion delocalizes phosphatidylinositol bisphosphate and inhibits hormone-stimulated phosphatidylinositol turnover. *J. Biol. Chem.* 273:22298–22304.

Pourati, J., A. Maniotis, D. Spiegel, J. L. Schaffer, J. P. Butler, J. J. Fredberg, D. E. Ingber, D. Stamenovic, and N. Wang. 1998. Is cytoskeletal tension a major determinant of cell deformability in adherent endothelial cells? *Am. J. Physiol. Cell Physiol.* 274:C1283–C1289.

Romanenko, V. G., G. H. Rothblat, and I. Levitan. 2002. Modulation of endothelial inward rectifier K^+ current by optical isomers of cholesterol. *Biophys. J.* 83:3211–3222.

Rotsch, C., and M. Radmacher. 2000. Drug-induced changes of cytoskeletal structure and mechanics in fibroblasts: an atomic force microscopy study. *Biophys. J.* 78:520–535.

Sato, M., D. P. Theret, L. T. Wheeler, N. Ohshima, and R. M. Nerem. 1990. Application of the micropipette technique to the measurement of cultured porcine aortic endothelial cell viscoelastic properties. *J. Biomech. Eng.* 112:263–268.

Simons, K., and E. Ikonen. 1997. Functional rafts in cell membranes. *Nature.* 387:569–572.

Sokoloff, L., and G. H. Rothblat. 1974. Sterol to phospholipid molar ratios of L cells with qualitative and quantitative variations of cellular sterol. *Proc. Soc. Exp. Biol. Med.* 146:1166–1172.

Spector, I., N. R. Shochet, D. Blasberger, and Y. Kashman. 1989. Latrunculins—novel marine macrolides that disrupt microfilament organization and affect cell growth. I. Comparison with cytochalasin D. *Cell Motil. Cytoskeleton.* 13:127–144.

Stahlhut, M., and B. van Deurs. 2000. Identification of filamin as a novel ligand for caveolin-1: evidence for the organization of caveolin-1-associated membrane domains by the actin cytoskeleton. *Mol. Biol. Cell.* 11:325–337.

Stockton, B. W., and I. C. P. Smith. 1976. A deuterium NMR study of the condensing effect of cholesterol on egg phosphatidylcholine bilayer membranes. *Chem. Phys. Lipids.* 17:251–263.

Theret, D. P., M. J. Levesque, F. Sato, R. M. Nerem, and L. T. Wheeler. 1988. The application of a homogenous half-space model in the analysis of endothelial cell micropipette measurements. *J. Biomech. Eng.* 110:190–199.

Wu, H. W., T. Kuhn, and V. T. Moy. 1998. Mechanical properties of L929 cells measured by atomic force microscopy: effects of anticytoskeletal drugs and membrane cross linking. *Scanning.* 20:389–397.

Xu, X., and E. London. 2000. The effect of sterol structure on membrane lipid domains reveals how cholesterol can induce lipid domain formation. *Biochemistry.* 39:843–849.

Yeagle, P. L. 1985. Cholesterol and the cell membrane. *Biochim. Biophys. Acta.* 822:267–287.

Yin, H. L., and P. A. Janmey. 2003. Phosphoinositide regulation of the actin cytoskeleton. *Annu. Rev. Physiol.* 65:761–789.

Zhang, G., M. Long, Z. Z. Wu, and W. Q. Yu. 2002. Mechanical properties of hepatocellular carcinoma cells. *World J Gastroenterol.* 8:243–246.